

# Global seismic damage assessment of high-rise hybrid structures

Xilin Lu, Zhihua Huang\* and Ying Zhou

*State Key Laboratory of Disaster Reduction in Civil Engineering, Tongji University  
Shanghai 200092, P.R. China*

*(Received July 3, 2009, Accepted November 21, 2010)*

**Abstract.** Nowadays, many engineers believe that hybrid structures with reinforced concrete central core walls and perimeter steel frames offer an economical method to develop the strength and stiffness required for seismic design. As a result, a variety of such structures have recently been applied in actual construction. However, the performance-based seismic design of such structures has not been investigated systematically. In the performance-based seismic design, quantifying the seismic damage of complete structures by damage indices is one of the fundamental issues. Four damage states and the final softening index at each state for high-rise hybrid structures are suggested firstly in this paper. Based on nonlinear dynamic analysis, the relation of the maximum inter-story drift, the main structural characteristics, and the final softening index is obtained. At the same time, the relation between the maximum inter-story drift and the maximum roof displacement over the height is also acquired. A double-variable index accounting for maximum deformation and cumulative energy is put forward based on the pushover analysis. Finally, a case study is conducted on a high-rise hybrid structure model tested on shaking table before to verify the suggested quantities of damage indices.

**Keywords:** high-rise hybrid structures; performance-based seismic design; global seismic damage assessment; final softening index; maximum inter-story drift; damage index with double variables.

---

## 1. Introduction

The hybrid structure with reinforced concrete central core walls and perimeter steel frames is an efficient type of structural system up to a certain height. The predominant lateral load resistance is provided by concrete cores while the steel frames surrounding the cores are generally designed mainly for gravity load. In the United States of America, the studies on seismic performance of such structure has been funded by the National Science Foundation (NSF) as part of the US-Japan Cooperative Research Program on Earthquake Engineering, Phase 5 on Composite and Hybrid structures (Wallace and Wada 2000). Performance-based seismic design (PBSD) of structures is becoming a preferred seismic design method during recent years. However, the PBSD of hybrid structures has not been investigated systematically. In PBSD, an accurate prediction of damage resulting from a seismic event is of prime importance. Hence, it is necessary to express damage in a quantitative form. Damage indices have been developed to provide a way to quantify the seismic damage numerically. Damage indices can be classified as local and global indices. Local indices reflect the damage of elements or storeys while global indices represent the damage of complete

---

\* Corresponding author, Ph.D., E-mail: [huangzhihua1981@163.com](mailto:huangzhihua1981@163.com)

structures. Global indices can be defined as weighted averages of local indices or defined in terms of global parameters which are used as indicators of damage.

Global indices can be classified based on the category of the global parameters used in them. The first category of global parameters uses deformation of structures as a damage indicator. The inter-story drift, defined as the maximum relative displacement between two storeys normalized to the storey height, is the most well-known index in this category (Sozen 1980). Global indices based on modal parameters are another group of indices. It is known that damage usually causes an increase in the natural period of a structure. Softening indices are used to relate changes in the first few natural periods of a structure to the level of damage it has incurred (Dipasquale 1989). Lakshmanan *et al.* (2007) present an analytical method of quantification and location of seismic damage, through system identification methods based on time period. To overcome the analytical difficulties in the calculation of the change in period as a measure of damage, a new approach for determining the change in stiffness of the structure was put forward by Ghobarah (1999). The best-known and most widely used global indices are based on maximum deformation and cumulative energy. Park and Ang (1985) suggested a local damage index which consists of a simple linear combination of normalized deformation and energy absorption. This index was then improved to estimate the damage of bridge columns, steel moment frames, special moment resisting frames and 1D structure by different researchers (Stone and Taylor 1993, Estekanchi and Arjomandi 2007, Zhang *et al.* 2007, Jehel *et al.* 2010).

The objective of this paper is to quantify the seismic damage of high-rise hybrid structures by different global indices, such as maximum inter-storey drift, final softening index and double-variable index by considering the maximum deformation and cumulative energy. The work of this paper can develop guidance to help engineers in choosing appropriate global indices according to the demand of private owners and the global parameters obtained as measures of damage by the selected nonlinear analysis programs.

## 2. Global indices of high-rise hybrid structures

### 2.1 Indices based on modal parameters

The first step in PBSO is the selection of seismic performance objectives for the design. A performance objective is a coupling of expected performance level with expected level of seismic ground motions. A performance level is a complete description of an overall damage state. Four damage states for high-rise hybrid structures are identified in this paper. These damage states are: (a) fully operational; (b) operational; (c) life safety; and (d) near collapse. Based on the shaking table model test of high-rise hybrid structures (Lu *et al.* 2008) and engineering experience, fundamental frequency and equivalent stiffness degradation at each damage state are shown in Table 1. The final softening index  $D_F$  calculated by Eq. (1) at each damage state are also list in Table 1.

Table 1 Fundamental frequency and equivalent stiffness degradation as well as final softening index at each damage state

Damage state	Fully operational	Operational	Life safety	Near collapse
Fundamental frequency degradation (%)	$\leq 5$	5~10	10~30	30~50
Equivalent stiffness degradation (%)	$\leq 10$	10~20	20~50	50~75
$D_F$	$\leq 0.1$	0.10~0.20	0.20~0.50	0.50~0.75



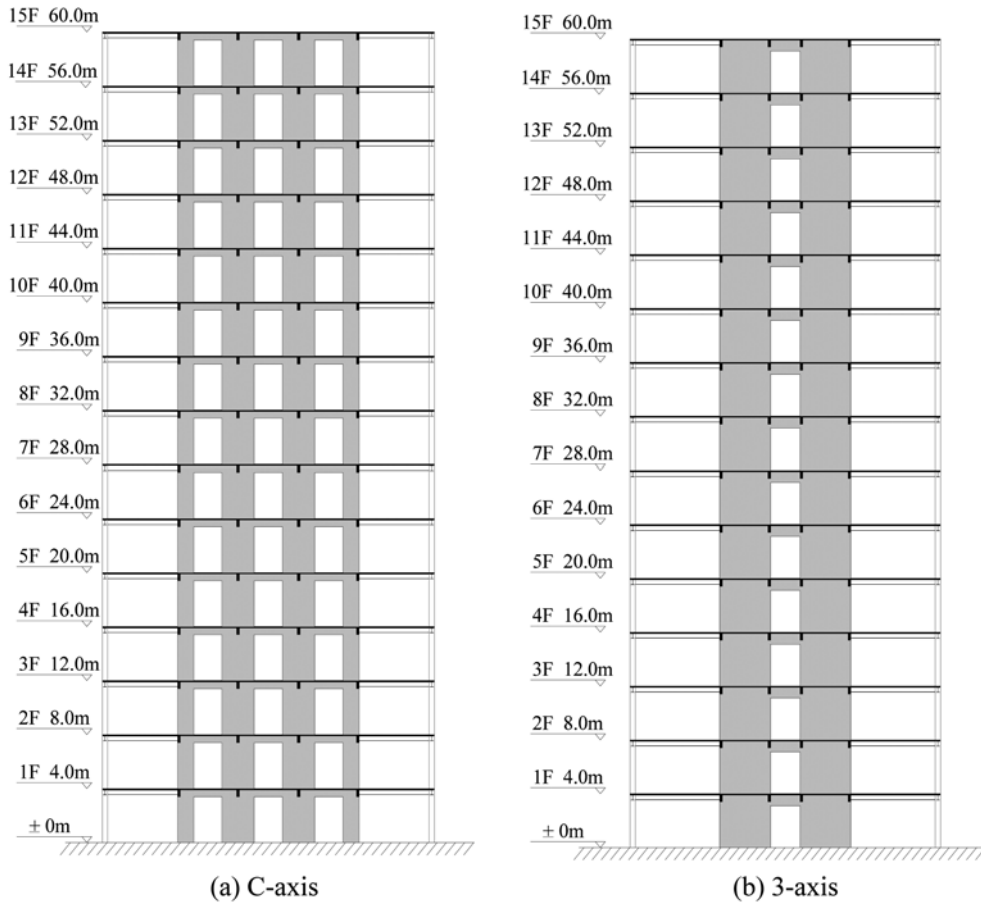


Fig. 2 Profiles of group 15F

Table 2 Parameters of group 15F

Structure	15FM1	15FM2	15FM3
Steel column	400×400×16	500×500×25	400×400×16
L-A	400×250×10×16	500×350×14×22	400×250×10×16
L-B	350×230×10×14	450×350×12×18	350×230×10×14
L-C	350×200×10×12	450×300×12×16	350×200×10×12
WX-1(2)		200	400
WY-1		1~3F: 220; 4~15F: 200	1~3F: 440; 4~15F: 400
WY-2		200	400
Coupling beam		LL-1: 400; LL-2: 750; LL-3: 400	
$\lambda_x$	0.62	1.07	0.44
$\lambda_y$	0.58	1.00	0.41
$E_u$ (kN·m)	7921	9043	10247

Table 3 Parameters of group 20F

Structure	20FM1	20FM2	20FM3
Steel column	500×500×20	650×650×30	500×500×20
L-A	400×300×12×20	550×400×16×26	400×300×12×20
L-B	400×250×10×18	500×350×14×26	400×250×10×18
L-C	400×200×10×14	500×300×14×20	400×200×10×14
WX-1(2)		200	400
WY-1		1~12F: 250; 13~20F: 200	1~12F:500;13~20F:400
WY-2		200	400
Coupling beam beams		1~12F: 800; 13~20F: 600	
$\lambda_x$	1.04	1.86	0.74
$\lambda_y$	0.94	1.70	0.67
$E_u$ (kN·m)	12361	12394	17242

Table 4 Parameters of group 25F

Structure	25FM1	25FM2	25FM3
Steel column	550×550×25	700×700×40	550×550×25
L-A	450×350×12×22	600×450×18×32	450×350×12×22
L-B	400×300×12×20	550×400×14×28	400×300×12×20
L-C	400×250×10×16	500×350×14×24	400×250×10×16
WX-1		1~10F: 300; 11~15F: 250; 16~25F: 200	1~10F: 600; 11~15F: 500; 16~25F: 400
WX-2		200	400
WY-1(2)		1~10F: 350; 11~15F: 300; 16~20F: 250; 21~25F: 200	1~10F: 700; 11~15F: 600; 16~20F: 500; 21~25F: 400
Coupling beam		LL-1: 800; LL-2: 1000; LL-3: 800	
$\lambda_x$	1.22	2.21	0.86
$\lambda_y$	1.20	2.15	0.85
$E_u$ (kN·m)	20741	37020	28525

span. It results in concentrated nonlinear deformation at element-end or in the spring. A column element is idealized by the multi-axial spring model which has a line element and two multi-axial spring elements at the column-end (Fig. 3). The multi-axial spring model allows for the interactions among the biaxial bending moments and the varying axial load in column element. A wall element is idealized by the fiber model (Fig. 4) that based on the material stress-strain relationships. There are two fiber slices considered at the base and top critical sections. Linear distribution of the element flexibility between the two fiber slices is assumed.

### 2.1.3 Ground motions

A series of nonlinear dynamic analyses were performed using several ground motions. The selected ground motions are El Centro record of the 1940 Imperial Valley earthquake (component 1: El Centro EW; component 2: El Centro NS), the 1952 Taft earthquake (component 1: Taft N21E; component 2: Taft S69E), the 1995 Kobe earthquake (component 1: Kobe EW; component 2: Kobe NS), the 1971 San Fernando earthquake (component 1: San Fernando S090; component 2: San

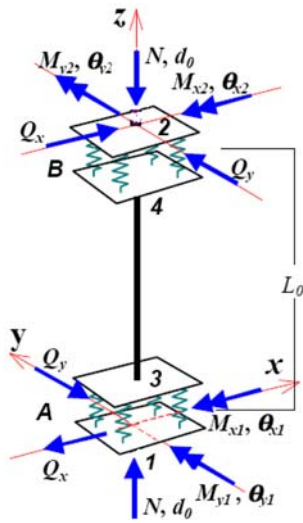


Fig. 3 Multi-spring model

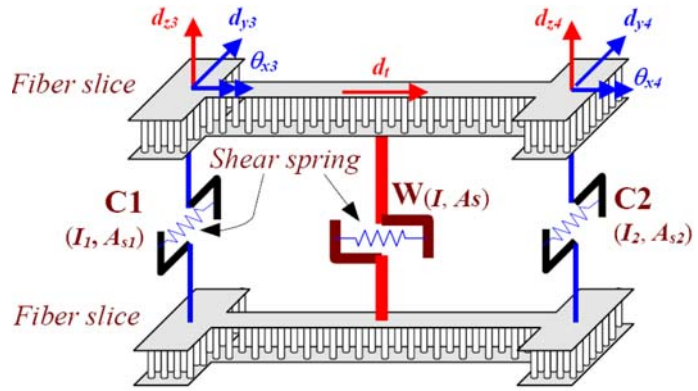


Fig. 4 Fiber model for 3D wall element

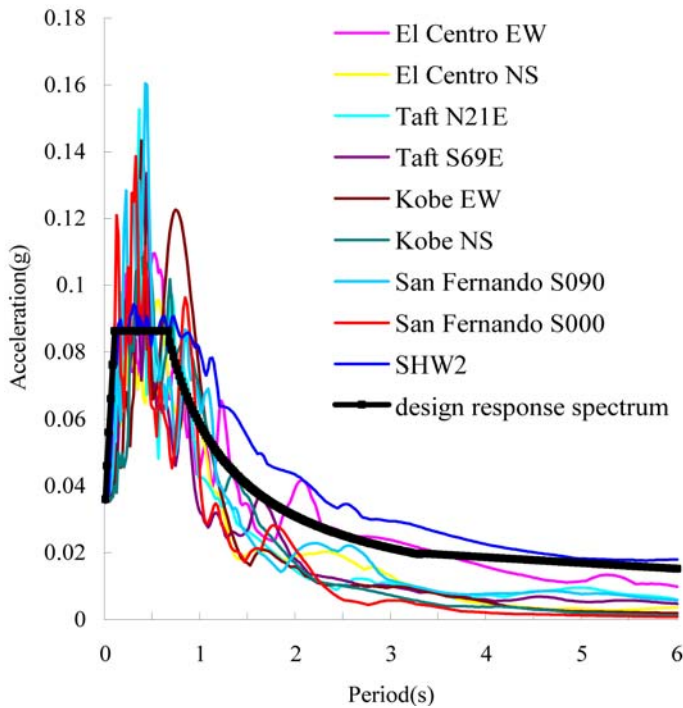


Fig. 5 Elastic response spectra

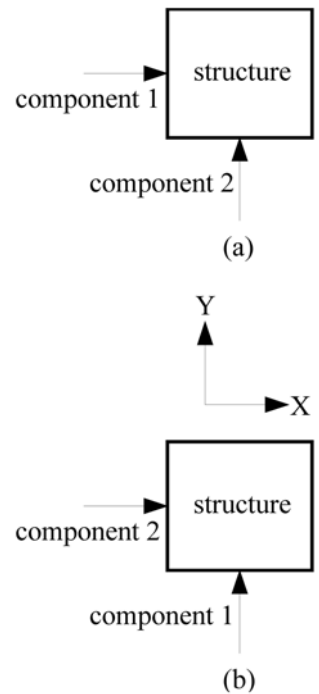


Fig. 6 2-D ground motion

Fernando S000) and Shanghai artificial accelerogram (SHW2 2003). The last one, specified for the particular soil condition, is 1-D wave, while the others are 2-D wave. The elastic response spectra of selected ground motions are shown in Fig. 5. Each 2-D ground motion was input twice: once in the principal direction  $X$  and once in  $Y$  (see Fig. 6). The peak acceleration ratio of the principal direction to the other direction is designed to be 1 to 0.85.

2.1.4 The final softening indices of high-rise hybrid structures

Figs. 7 and 8 show the final softening index versus peak ground acceleration (PGA) when group 15F subjected to various earthquakes scaled to different PGA levels. Figs. 9 and 10 show the final

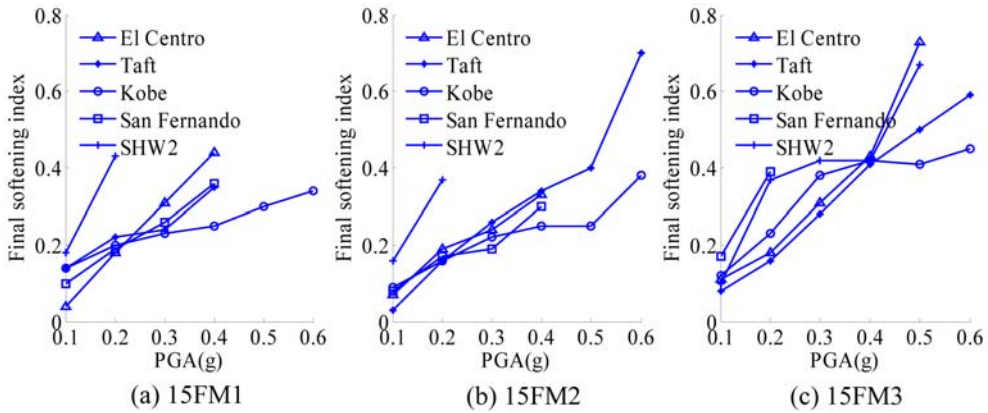


Fig. 7 The final softening index variation with PGA for group 15F when input in the principal direction X

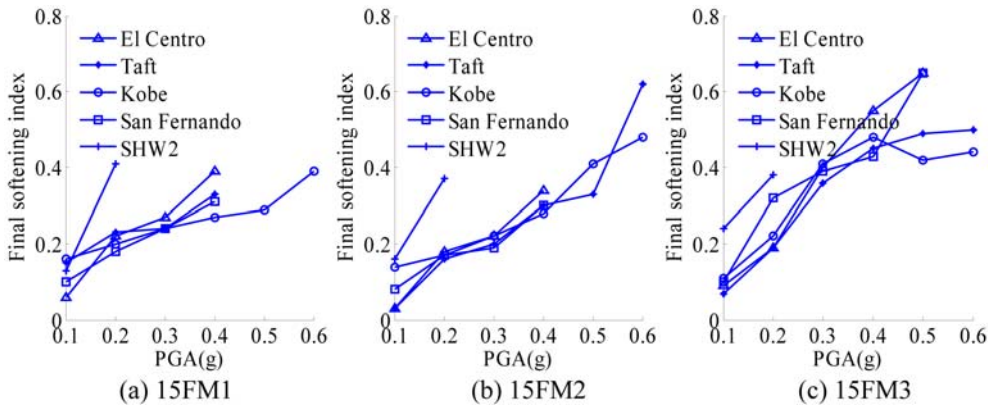


Fig. 8 The final softening index variation with PGA for group 15F when input in the principal direction Y

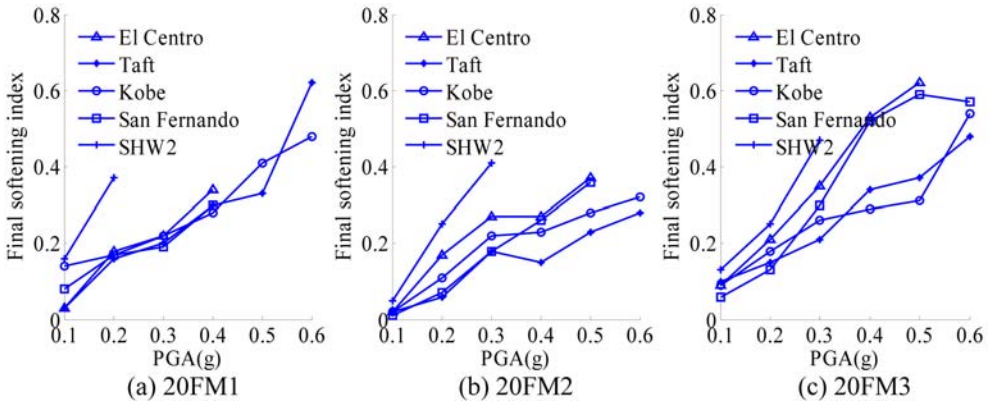


Fig. 9 The final softening index variation with PGA for group 20F when input in the principal direction X

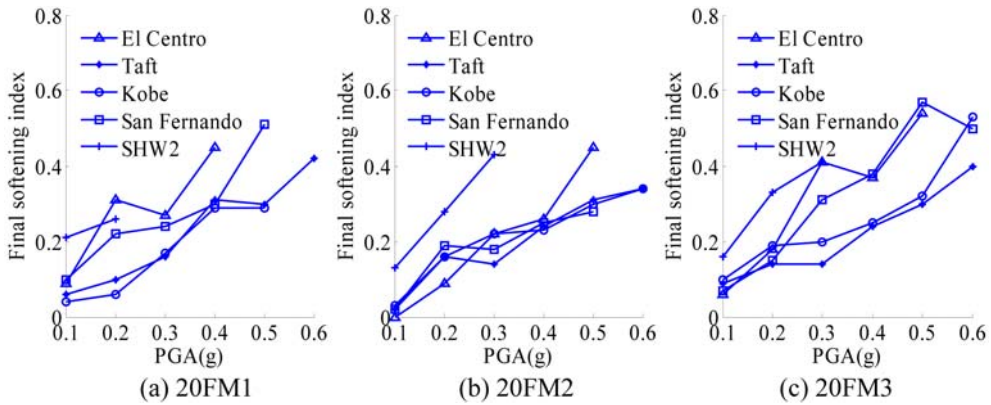


Fig. 10 The final softening index variation with PGA for group 20F when input in the principal direction Y

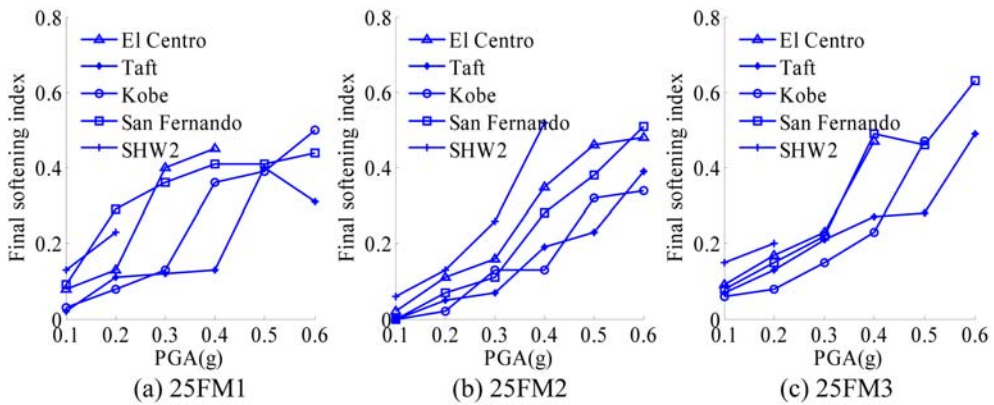


Fig. 11 The final softening index variation with PGA for group 25F when input in the principal direction X

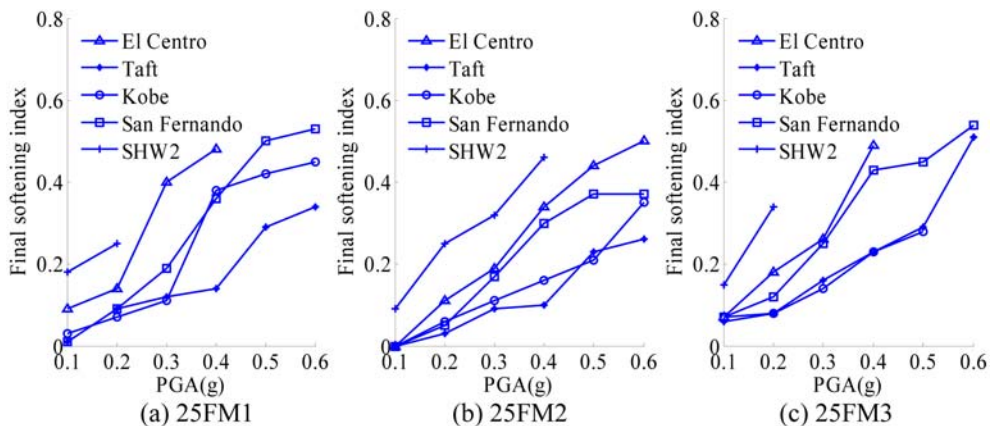


Fig. 12 The final softening index variation with PGA for group 25F when input in the principal direction Y

softening index versus PGA for group 20F. Figs. 11 and 12 show the final softening index versus PGA for group 25F. In some cases, the final softening index was found to decrease with increasing PGA level which is not physically correct. However, this is mainly due to the analytical difficulties

in determining the final period. The period calculated at the final step of the earthquake loading may be affected by the randomness of the instantaneous tangent stiffness which is significantly different in loading and unloading direction.

## 2.2 Indices based on maximum deformation

The maximum inter-storey drift  $\theta_{max}$  is an observable response quantity that relates to both the structural and non-structural performance of a building subjected to earthquake motions. Hence,  $\theta_{max}$  is chosen as a basic parameter to control the performance of high-rise hybrid structures in this study. Fig. 13 shows the maximum inter-storey drift variation with the final softening index. Based on the statistical analysis of the data in this figure,  $\theta_{max}$  is then expressed as

$$\theta_{max} = 0.01105 \exp(D_F) + 0.000873 \lambda + 4.31 \times 10^{-5} H/B - 0.0114 \quad (3)$$

where  $H/B$  is the height-to-width ratio. With Eq. (3) and Table 1, the range of  $\theta_{max}$  at each damage

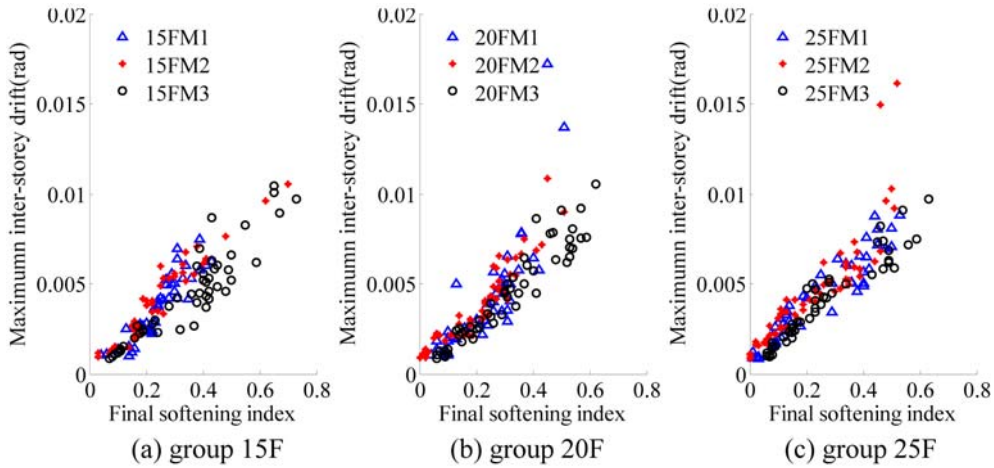


Fig. 13 The maximum inter-storey drift variation with the final softening index

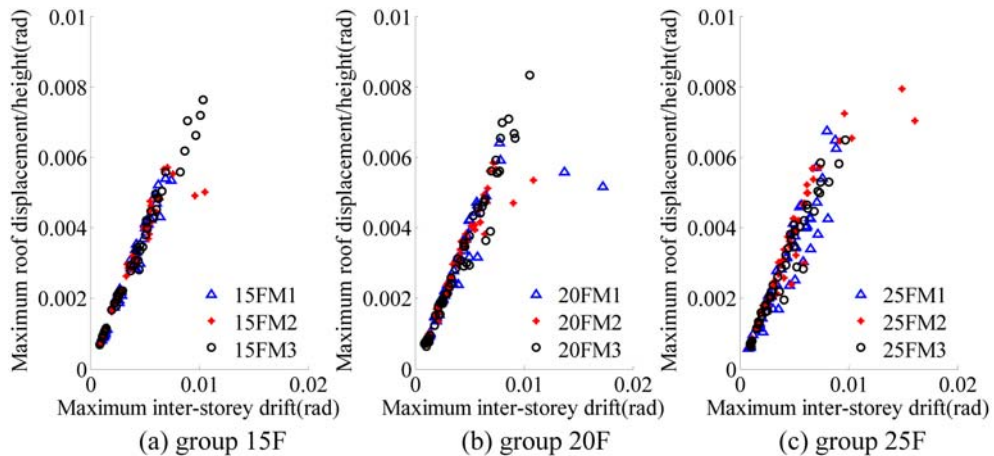


Fig. 14 The maximum roof displacement over the height variation with the maximum inter-storey drift

state can be obtained.

Fig. 14 illustrates the variation of the maximum roof displacement over the height  $U_{max}/H$  with the maximum inter-storey drift. From the figure, it can be seen that the  $U_{max}/H$  which is independent on the structural parameters  $\lambda$  and  $H/B$  can be related to  $\theta_{max}$  as

$$U_{max}/H = \theta_{max}/1.35 \quad (4)$$

### 2.3 Indices based on maximum deformation and cumulative energy

In this paper, the double-variable index  $D$  by considering the maximum deformation and cumulative energy is defined as

$$D = \alpha(U_{max}/U_u) + \beta(E_H/E_u) \quad (5)$$

where  $U_{max}$  and  $U_u$  are the maximum and ultimate displacement, respectively;  $E_H$  and  $E_u$  are the hysteretic and ultimate energy, respectively. In Eq. (5), the first variable represents the portion of the deformation while the second variable represents the portion of the energy. The contribution factors,  $\alpha$  and  $\beta$ , represent the contribution from the deformation and energy part, respectively.

#### 2.3.1 Deformation part

With Eqs. (3) and (4),  $U_u$  in the deformation part can be obtained. The value of  $D_F$  in Eq. (3) is assumed to be 0.75, which means that ultimate displacement is defined by 75% reduction (or 25% retention) of the equivalent stiffness (see Table 1). Fig. 15 shows the variation of the maximum displacement over the ultimate displacement  $U_{max}/U_u$  with the final softening index  $D_F$ .

#### 2.3.2 Energy part

The dynamic equilibrium equation of motion is

$$[M]\{\ddot{X}\} + [C]\{\dot{X}\} + [K]\{X\} = -[M]\{\ddot{X}_g\} \quad (6)$$

where  $[M]$  is the mass matrix,  $[C]$  is the damping matrix,  $[K]$  is the stiffness matrix  $\{\ddot{X}\}$  is the

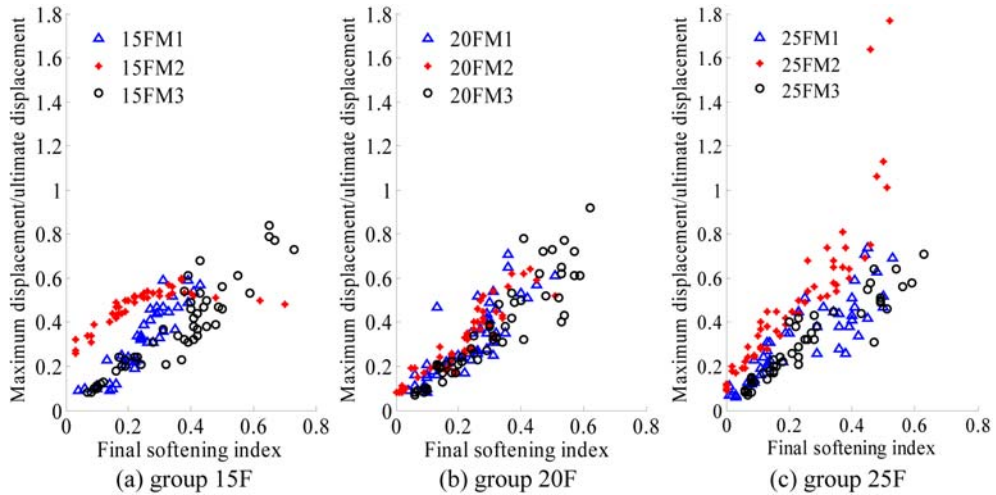


Fig. 15 The maximum displacement over the ultimate displacement variation with the final softening index

acceleration vector,  $\{\dot{X}\}$  is the velocity vector,  $\{X\}$  is the displacement vector; and  $\{\ddot{X}_g\}$  is the ground acceleration vector. Integrating both sides of the equation from time zero to time  $t_k$ , the energy balance equation is obtained as

$$\int_0^{t_k} \{\dot{X}\}^T [M] \{\ddot{X}\} dt = \int_0^{t_k} \{\dot{X}\}^T [C] \{\dot{X}\} dt + \int_0^{t_k} \{\dot{X}\}^T [K] \{X\} dt = - \int_0^{t_k} \{\dot{X}\}^T [M] \{\ddot{X}_g\} dt \quad (7)$$

or

$$E_K + E_D + E_S + E_H = E_I \quad (8)$$

where  $E_K$  is the kinetic energy;  $E_D$  is the damping energy,  $E_S$  is the elastic strain energy,  $E_I$  is the input energy. The energy terms can be simplified as follows

$$E_K = \int_0^{t_k} \{\dot{X}\}^T [M] \{\ddot{X}\} dt \quad (9)$$

$$E_D = \int_0^{t_k} \{\dot{X}\}^T [C] \{\dot{X}\} dt \quad (10)$$

$$E_S + E_H = \int_0^{t_k} \{\dot{X}\}^T [K] \{X\} dt \quad (11)$$

$$E_I = - \int_0^{t_k} \{\dot{X}\}^T [M] \{\ddot{X}_g\} dt \quad (12)$$

Due to the increasing nature of damping energy and hysteretic energy as time progresses, the maximum values of these energy forms generally occur at the end of the earthquake duration in the analysis. The kinetic energy and elastic strain energy are usually quite small because the earthquake ground motion has diminished and therefore not much energy is “stored” in the system (Wong and Pang 2005). Hence, the Eq. (8) can be written as

$$E_D(t_k) + E_H(t_k) \approx E_I(t_k) \quad (13)$$

This equation shows that input energy at time  $t_k$  can be decomposed into damping energy and hysteretic energy. The existence of the hysteretic energy in the equation indicates the damage of the structure due to earthquake motion. Fig. 16 shows the typical curves for individual items of the energy calculated by CANNY.

Much research (Niu and Ren 1996, Liu 2006) focuses on the methods to evaluate  $E_u$ . Unfortunately, the

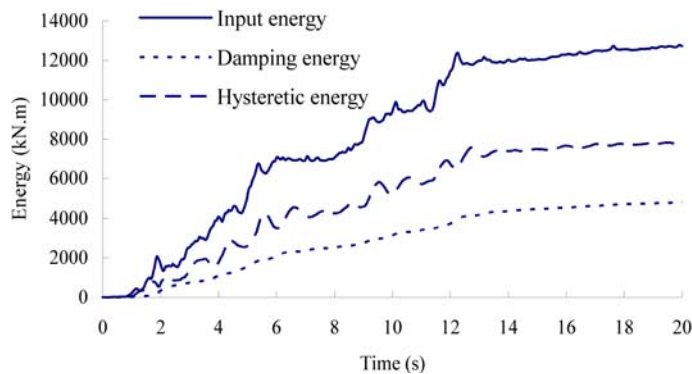
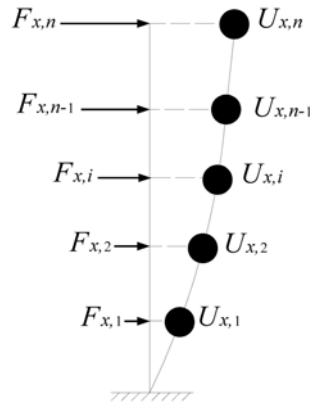


Fig. 16 Energy graph

Fig. 17 Deformation of an  $n$ -storey structure

current methods are simple but inaccurate or accurate but difficult to carry out. In this paper, a procedure developed to tackle the problem is organized in two phrases: first, a pushover analysis is used to obtain the force-displacement curve of each storey. In the pushover analysis, an inverted triangular load representing the lateral load distribution is performed along direction  $X$  and  $Y$  simultaneously. Second, according to the deformation of an  $n$ -storey structure (Fig. 17), the  $E_u$  is defined as

$$E_u = \sum_{i=1}^n (F_{x,i}U_{x,i} + F_{y,i}U_{y,i}) \quad (14)$$

where  $F_{x,i}$  and  $F_{y,i}$  are the force at  $i$ th storey level in direction  $X$  and  $Y$ , respectively;  $U_{x,i}$  and  $U_{y,i}$  are the displacement at  $i$ th storey level in direction  $X$  and  $Y$ , respectively. The ultimate energy for groups 15F, 20F and 25F is shown in Tables 2, 3 and 4, respectively.

Fig. 18 illustrates the variation of the hysteretic energy over the ultimate energy  $E_H/E_u$  with the final softening index  $D_F$ .

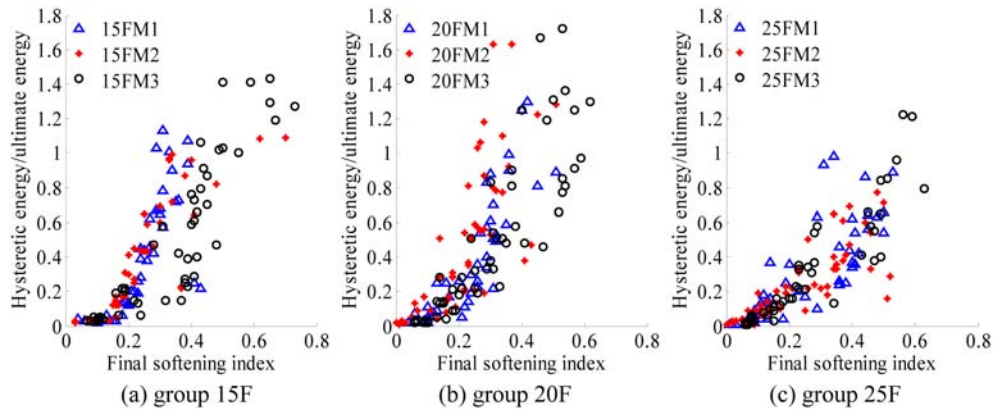


Fig. 18 The hysteretic energy over the ultimate energy variation with the final softening index

### 2.3.3 Contribution factors

The contribution factors,  $\alpha$  and  $\beta$ , are determined in such a way that the double-variable index is equal to the final softening index. The equation is expressed as

$$\alpha(U_{max}/U_u) + \beta(E_H/E_u) = D_F \quad (15)$$

The contribution factors,  $\alpha$  and  $\beta$ , are then calculated to be 0.36 and 0.20, respectively. Therefore, the double-variable index  $D$  can be written as

$$D = 0.36(U_{max}/U_u) + 0.20(E_H/E_u) \quad (16)$$

## 3. Case study

A 15-storey prototype structure was designed according to codes. The stiffness ratios,  $\lambda_x$  and  $\lambda_y$ , were obtained to be 0.65 and 0.63, respectively. With Eq. (14), the ultimate energy  $E_u$  was calculated to be 6055 kN·m. A 1/20 scale model of this structure (Fig. 18) was then tested on the shaking table to study its seismic behaviour. The test was carried out in 4 stages. The first stage represented frequent occurrence of intensity 7. In this stage, El Centro and San Fernando records were employed to perform the excitations firstly. After these test cases, a white noise case W4 was conducted. Then Pasadena record was input as the excitation four times. The four cases are: F7PXX, F7PYY, F7PXY, and F7PYX. At last, a white noise case W5 was conducted. The detailed



Fig. 19 Tested model

Table 5 Damage indices at each damage state

Damage state	Fully operational	Operational	Life safety	Near collapse
$D_F$	$\leq 0.1$	0.10~0.20	0.20~0.50	0.50~0.75
$\theta_{max}$	$\leq 1/680$	1/680~1/360	1/360~1/130	1/130~1/80
$D$	$\leq 0.1$	0.10~0.20	0.20~0.50	0.50~0.75

Table 6 Comparisons of test results and numerical analysis

	Test		Numerical analysis of prototype
	Model	Prototype	
$T_{ind}$ (s)	0.205	1.587	1.579
$T_{dam}$ (s)	0.222	1.717	1.616
$U_{max}$ (mm)	4.49	89.88	74.83
$U_{max}/H$		1/680	1/815
$\theta_{max}$		–	1/714
$E_H$ (kN·m)		–	41.6
$D_F$		0.14	0.05

test program is introduced by Shen and Lu (2008). The Damage indices at each damage state are shown in Table 5. For case F7PYX, the test results and numerical analysis are list in Table 6.

From Table 6, one can find that the value of  $D_F$  obtained from test results is significant different from the value from numerical analysis. However, this is mainly due to the analytical difficulties in considering the cumulative damage caused by the three cases before F7PYX for the nonlinear dynamic analysis. The double-variable index  $D$  given by Eq. (16) is

$$D = 0.36 \frac{U_{max}}{U_u} + 0.20 \frac{E_H}{E_u} = 0.36 \times \frac{1/815}{(1/80)/1.35} + 0.20 \times \frac{41.6}{6055} = 0.05 \quad (17)$$

According to the global indices  $D_F$ ,  $\theta_{max}$  and  $D$  acquired from the numerical analysis, the damage state of the structure can be defined as fully operational. In this state, only some RC coupling beams crack.

## 4. Conclusions

In this paper, the seismic damage of high-rise hybrid buildings is quantified by maximum inter-storey drift, final softening index and double-variable index. The paper aims at proposing the direct relation between the different indices and quantifying the indices at each damage state. Moreover, a 15-storey building is presented as an example to show the application of the damage indices. The relation between the three damage indices and their qualifications are summarized from the results of more than 500 nonlinear analyses using selected earthquake records. The example shows that obtained results are applicable with acceptable accuracy.

Damage indices are different when considering their applicability to different analysis methods. The maximum inter-storey drift can be applied in spectral and time-history analysis, while, final softening index and double-variable index are only applicable in time-history analysis. So, the last two damage indices are difficult to calculated, especially the double-variable index, which includes more sophisticated parameters.

The simple concept and ease of use makes the first selected index versatile for practical application. However, because the private owners are not accustomed to the engineering terminology, it is advisable for engineers to use the last two indices when they carry out the performance-based seismic design. These two damage indexes are calibrated to equal zero in no structural damage

range and to equal one in total structural damage range. In conclude, engineers could choose appropriate global damage indices according to the demand of private owners and the global parameters obtained as measures of damage by the selected nonlinear analysis programs.

## Acknowledgements

This work was supported by the Natural Science Foundation of China through grant No.90815029 and No.50708071.

## References

- DiPasquale, E. and Cakmak A.S. (1989), "On the relation between local and global damage indices", *Technical Report NCEER-89-0034*, State University of New York at Buffalo.
- Estekanchi, H. and Arjomandi, K. (2007), "Comparison of damage indexes in nonlinear time history analysis of steel moment frames", *Asian J. Civil Eng.*, **8**(6), 629-646
- Ghobarah, A., Abou-Elfath, H. and Biddah, Ashraf (1999), "Response-based damage assessment of structures", *Earthq. Eng. Struct. Dyn.*, **28**(1), 79-104.
- Jehel, P., Davenne, L., Ibrahimbegovic, A. and Leger, P. (2010), "Towards robust viscoelastic-plastic-damage material model with different hardenings/softenings capable of representing salient phenomena in seismic loading applications", *Comput. Concrete*, **7**(4), 365-386.
- Lakshmanan, N., Raghuprasad, B.K., Muthumani, K., Gopalakrishnan, N. and Sreekala, R. (2007), "Seismic damage estimation through measurable dynamic characteristics", *Comput. Concrete*, **4**(3), 167-186.
- Li, K.N. (2003), 3-Dimensional nonlinear static/dynamic structural analysis computer program CANNY-Technical Manual.
- Liu, Z.F. (2006), "Energy-based seismic design method and application in seismic evaluation of tall building hybrid structure", PhD thesis, Hunan University.
- Lu, X.L., Chen, L.Z., Zhou, Y. and Huang Z.H. (2008), "Shaking table model tests on a complex high-rise building with two towers of different height connected by trusses", *Struct. Des. Tall Spec. Build.* (in press)
- Niu, D.T. and Ren, L.J. (1996), "A modified seismic damage model with double variables for reinforced concrete structures", *Earthq. Eng. Eng. Vib.*, **16**(4), 44-54.
- Park, Y.J. and Ang, A.H-S. (1985), "Mechanistic seismic damage model for reinforced concrete", *J. Struct. Eng.*, **111**(4), 722-739.
- Shen, D.J. and Lu, X.L. (2008), "Shaking table test and analysis on seismic behavior of steel-concrete hybrid structure for high rise buildings", *Proceedings of the 14<sup>th</sup> World Conference on Earthquake Engineering*, Beijing, October, Paper ID. 05-06-0162.
- Sozen, M.A. (1980), "Review of earthquake response of reinforced concrete buildings with a view to drift control", State-of-the-Art in Earthquake Engineering, *Proceedings of the 7<sup>th</sup> World Conference on Earthquake Engineering*, Istanbul, September, 119-174.
- Stone, W.C. and Taylor, A.W. (1993), "Seismic performance of circular bridge column designed in accordance with AASHTO/CALTRANS standards", *NIST Buildings Science Series 170*, National Institute of Standard and Technology, Gaithersburg MD.
- Wallace, J.W. and Wada, A. (2000), "Hybrid wall system: US-Japan research", *Proceedings of the 12<sup>th</sup> World Conference on Earthquake Engineering*, Auckland, February, Paper No. 2619.
- Wong, K.K.F. and Pang, M. (2007), "Energy density spectra in actively controlled inelastic structures", *Struct. Control Health Monit.*, **14**, 261-278.
- Zhang, X., Wong, K.K.F. and Wang, Y. (2007), "Performance assessment of moment resisting frames during earthquakes based on the force analogy method", *J. Struct. Eng.*, **29**(10), 2792-2802.